

## Phase transitions in quantum dots

H.-M. Müller and S. E. Koonin

W. K. Kellogg Radiation Laboratory, 106-38, California Institute of Technology, Pasadena, California 91125

(Received 16 July 1996)

We perform Hartree-Fock calculations to show that quantum dots (i.e., two-dimensional systems of up to twenty interacting electrons in an external parabolic potential) undergo a gradual transition to a spin-polarized Wigner crystal with increasing magnetic-field strength. The phase diagram and ground-state energies have been determined. We tried to improve the ground state of the Wigner crystal by introducing a Jastrow ansatz for the wave function and performing a variational Monte Carlo calculation. The existence of so-called magic numbers was also investigated. Finally, we also calculated the heat capacity associated with the rotational degree of freedom of deformed many-body states. [S0163-1829(96)04544-4]

### I. INTRODUCTION

Quantum dots have been the subject of recent intense experimental and theoretical research. The interest in these nanostructures arises not only from possible new technological applications, but also from the desire to understand the fundamental physical problem of a few ( $m \leq 300$ ) interacting electrons in an external potential and a strong magnetic field.

In a weak magnetic field electrons form a rotationally symmetric state by occupying the lowest Fock-Darwin levels. With increasing magnetic field, the behavior is determined by three basic mechanisms: the spin alignment of the electrons (eventually resulting in a spin-polarized system), the Pauli principle (which causes the ground states of the system to occur with certain "magic numbers" of the total angular momentum<sup>1,2</sup>), and finally the Coulomb interaction. This latter makes the electron droplet susceptible to edge excitations and bulk instabilities, as the electron-electron interaction favors a larger area.<sup>3,4</sup>

The scenario above assumes an unbroken rotational symmetry. Questions concerning a high-field transition to so-called Wigner molecules and crystals, in which electrons occupy fixed sites in a rotating frame and are therefore localized, have been investigated by Maksym<sup>2</sup> and Bolton and Rössler.<sup>5</sup> Maksym considers a "large angular momentum limit" of systems of up to five electrons and describes only excited states of integer angular momentum. He speculates on the existence of ground-state Wigner molecules in the large-field limit. Bolton and Rössler simulated up to 40 classical interacting point charges in an external parabolic potential.

In this paper we consider the ground-state properties of up to 20 electrons in the limit of a strong magnetic field. We treat the full quantal problem by solving the Hartree-Fock equations for the two-dimensional electron gas. After a brief description of the well-known phases of the rotationally symmetric case as they appear in the Hartree-Fock approximation, we present the gradual transition towards a Wigner molecule and crystal; the various spatial configurations are shown and the shell structure is compared to that of the classical calculation.<sup>5</sup> We further describe a variational Monte

Carlo calculation that we performed to improve the wave function by a Jastrow ansatz. Finally, we investigate the rotational spectra associated with the breaking of the continuous rotational symmetry; the heat capacity associated with this new rotational degree of freedom is calculated.

### II. THEORY

We consider  $m$  electrons of effective mass  $m^*$  in a plane  $(x, y)$  confined by an external parabolic potential,  $V(r) = \frac{1}{2}m^*\omega_0^2 r^2$ , and subject to a strong magnetic field  $\vec{B} = B_0 \vec{e}_z$ . The Hamiltonian for such a system is

$$\hat{H} = \sum_{i=1}^m \frac{1}{2m^*} \vec{\Pi}_i^2 + \sum_{i=1}^m \frac{1}{2} m^* \omega_0^2 (x_i^2 + y_i^2) + \sum_{i=1}^m \frac{g^* \mu_B \vec{B} \cdot \vec{S}_i}{\hbar} + \sum_{i < j} \frac{e^2}{\epsilon |\vec{r}_i - \vec{r}_j|}, \quad (1)$$

where  $\vec{\Pi}_i = (\hbar/i) \vec{\nabla}_i + (e/c) \vec{A}(\vec{r}_i)$  is the kinetic momentum of the  $i$ th electron in the vector potential  $\vec{A}(\vec{r}_i) = (B_0/2)(-y_i, x_i, 0)$ . We include the spin degree of freedom of the electrons,  $\vec{S}_i$  (which implies the addition of the Zeeman energy with  $g^* \approx 0.54$  as the effective  $g$  factor for the material GaAs), but neglect any spin-orbit interaction. (An order-of-magnitude estimate for the magnetic-field strength induced by the circular motion of an electron with an angular momentum of  $\hbar$  at a distance of  $l_0 \sim 1.0 \times 10^{-6}$  cm is only  $e\hbar/m^*cl_0^3 \approx 2.8 \times 10^{-5}$  T.) Defining the frequencies  $\omega_c = eB_0/m^*c$  and  $\omega(B_0) = \sqrt{\omega_0^2 + \frac{1}{4}\omega_c^2}$ , we rewrite the coordinates as dimensionless complex variables,  $z_i = (1/l_0)(x_i - iy_i)/\sqrt{2}$ , where  $l_0 = \sqrt{\hbar/m^*\omega(B_0)}$  is the magnetic length, to obtain

$$\begin{aligned}
\hat{H} &= \sum_{i=1}^m -\frac{\hbar^2}{m^*} \left( \frac{1}{l_0^2} \partial_{z_i} \partial_{\bar{z}_i} \right) + m^* \omega^2 (B_0) l_0^2 |z_i|^2 \\
&+ \frac{\hbar}{2} \omega_c (\bar{z}_i \partial_{\bar{z}_i} - z_i \partial_{z_i}) + \sum_{i=1}^m \frac{g^* \mu_B \vec{B} \cdot \vec{S}_i}{\hbar} \\
&+ \sum_{i<j} \frac{e^2}{\epsilon \sqrt{2} l_0 |z_i - z_j|} \\
&= \sum_{i=1}^m \hat{H}_0(z_i, \vec{S}_i) + \frac{e^2}{\epsilon \sqrt{2} l_0} \sum_{i<j} \frac{1}{|z_i - z_j|}. \quad (2)
\end{aligned}$$

$\hat{H}_0$  is the single-particle Hamiltonian whose eigenfunctions will form the basis states for the Hartree-Fock calculation. For the spatial part of  $\hat{H}_0$  we define

$$\begin{aligned}
a^\dagger &= \frac{1}{\sqrt{2}} (\bar{z} - \partial_z), & b^\dagger &= \frac{1}{\sqrt{2}} (z - \partial_{\bar{z}}), & a &= \frac{1}{\sqrt{2}} (z + \partial_{\bar{z}}), \\
b &= \frac{1}{\sqrt{2}} (\bar{z} + \partial_z) \quad (3)
\end{aligned}$$

with  $[a, a^\dagger] = [b, b^\dagger] = 1$  and write

$$\begin{aligned}
\hat{H}_0(z) &= \hbar \omega (B_0) (a^\dagger a + b^\dagger b + 1) - \frac{1}{2} \hbar \omega_c (b^\dagger b - a^\dagger a) \\
&= \hbar \omega (B_0) (2a^\dagger a + \mathcal{L} + 1) - \frac{1}{2} \hbar \omega_c \mathcal{L}, \quad (4)
\end{aligned}$$

where  $\mathcal{L} := b^\dagger b - a^\dagger a$  is the angular momentum of the particle. The eigenvalues of the single-particle Schrödinger equation  $\hat{H}_0 \Psi_{nk} = \epsilon_{nk} \Psi_{nk}$ ,  $\epsilon_{nk} = \hbar \omega (B_0) \{2n + |k| + 1\} - \frac{1}{2} \hbar \omega_c k$ , indicate that for strong magnetic fields, e.g.,  $B_0 \approx 10$  T, one has  $\hbar \omega_c \approx 17$  meV and  $\hbar \omega (B_0) \approx 9$  meV (assuming  $\hbar \omega_0 = 3$  meV), and all particles occupy the Fock-Darwin states with  $n=0$ :

$$\begin{aligned}
\Delta \epsilon &= \epsilon_{n=0L} - \epsilon_{n=0L-1} \approx 0.5 \text{ meV} \ll \epsilon_{n=0L} - \epsilon_{n=1L} \\
&\approx 18 \text{ meV}.
\end{aligned}$$

We therefore restrict our calculation to the  $n=0$  level, which resembles the lowest Landau level if the external potential had been switched off. The eigenfunctions are

$$\bar{v}_{abcd} = \frac{e^2}{\epsilon \sqrt{2} l_0} \times \begin{cases} \langle ab | \frac{1}{|z_i - z_j|} | cd \rangle - \langle ab | \frac{1}{|z_i - z_j|} | dc \rangle & \text{if } s_c = s_d \\ \langle ab | \frac{1}{|z_i - z_j|} | cd \rangle & \text{if } s_c \neq s_d. \end{cases} \quad (6)$$

To minimize Eq. (5), we vary with respect to  $\rho$ ,  $\delta E^{\text{HF}} / \delta \rho = 0$ , with the constraints that we stay within the set of Slater determinants ( $\rho^2 = \rho$ ) and conserve the number of particles ( $\text{tr} \rho = m$ ) resulting in the matrix diagonalization problem

$$\begin{aligned}
\sum_j h_{ij} D_{jk} &= \sum_j (t_{ij} + \Gamma_{ij}) D_{jk} \\
&= \sum_j \left( t_{ij} + \sum_{l'l''} \bar{v}_{il'l''} \rho_{l'l''} \right) D_{jk} = \epsilon_k D_{ik}, \quad (7)
\end{aligned}$$

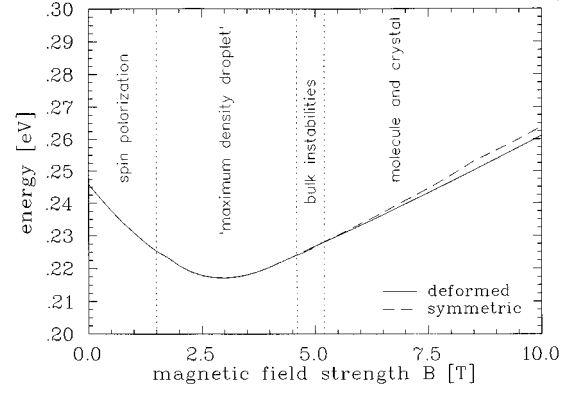


FIG. 1. Ground-state energy of the Wigner molecule (solid line) and lowest rotationally symmetric state (dashed line) for ten electrons.

$\Psi_k \sim z^k \exp(-|z|^2)$  and are identical to the usual form  $\phi_k \sim e^{-ik\varphi} r^k L_0^{|k|}(r) \exp(-r^2/2l_0^2)$ ,  $L_0^{|k|}(r)$  being the Laguerre polynomial of degree zero.

In the Hartree-Fock calculation, we minimize the Hartree-Fock energy

$$\begin{aligned}
E^{\text{HF}} &= \langle \Phi | \hat{H} | \Phi \rangle = \sum_{l_1 l_2} t_{l_1 l_2} \langle \Phi | c_{l_1}^\dagger c_{l_2} | \Phi \rangle \\
&+ \frac{1}{4} \sum_{l_1 l_2 l_3 l_4} \bar{v}_{l_1 l_2 l_3 l_4} \langle \Phi | c_{l_1}^\dagger c_{l_2}^\dagger c_{l_4} c_{l_3} | \Phi \rangle \\
&= \sum_{l_1 l_2} t_{l_1 l_2} \rho_{l_2 l_1} + \frac{1}{2} \sum_{l_1 l_2 l_3 l_4} \rho_{l_3 l_1} \bar{v}_{l_1 l_2 l_3 l_4} \rho_{l_4 l_2} \quad (5)
\end{aligned}$$

with  $\rho_{l_1 l_2} = \langle \Phi | c_{l_2}^\dagger c_{l_1} | \Phi \rangle$  being the density matrix and  $|\Phi\rangle$  being a Slater determinant.  $c_l^\dagger$  creates a fermion in the state  $\Psi_l$ , while its Hermitian conjugate  $c_l$  destroys it. The indices  $l_i = (k_i, s_i)$  run over all orbital states  $k$ , as well as the spin degree of freedom  $s = \{+\frac{1}{2}, -\frac{1}{2}\}$ .  $t_{l_1 l_2} = \langle \Psi_{l_1} | \hat{H}_0 | \Psi_{l_2} \rangle = \epsilon_{k_1} \delta_{k_1 k_2} + (-1)^{s_1+1/2} (g^* \mu_B B_0 / 2) \delta_{s_1 s_2}$  is the single-particle matrix element of the Hamiltonian and  $\bar{v}$  the antisymmetrized Coulomb matrix element,

where  $\Gamma$  is the so-called mean field. The eigenvectors  $\vec{D}_k$  of  $h$  represent the new single-particle states  $\{k\}$ , which are to be occupied according to the energies  $\epsilon_k$ . Equation (7) has to be solved self-consistently, since  $\rho_{ll'} = \sum_{i=1}^m D_{li} D_{l'i}^*$ .

We use the Fock-Darwin representation in our calculation and take into account up to 200 single-particle states (including spin). We tested our code by comparison with the results of Pfannkuche, Gudmundsson, and Maksym<sup>6</sup> and Bolton.<sup>7</sup> Although Pfannkuche, Gudmundsson, and Maksym describe quantum dot helium in a model space that is different from

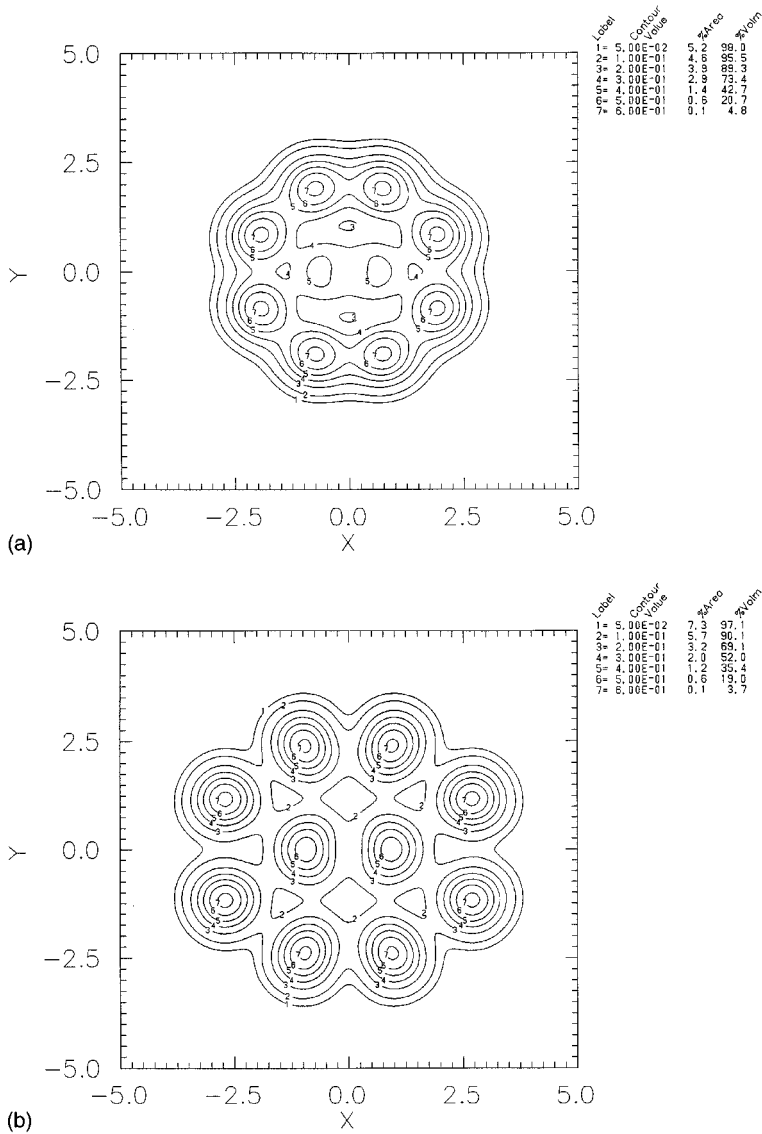


FIG. 2. The electron density distribution for  $m=10$  electrons. The upper panel shows the solution at  $B_0=6$  T, the lower at  $B_0=10$  T.

ours (they included  $n \neq 0$  states in their calculation), our ground-state energies of total angular momentum  $J=1$  for  $0 \leq B_0 \leq 5$  T coincide with their Hartree-Fock calculation within less than 2%, and the  $J=0$  ground-state energies agree with less than 5%. As one can see in Table I of Ref. 6, the  $n \neq 0$  coefficients in their  $J=0$  ground state are larger than in their  $J=1$  ground state, so that the  $n \neq 0$  space is more significant for those magnetic-field strengths. Similar results are obtained if we compare our results to the fixed node Monte Carlo calculation of Ref. 7. In the spin-polarized case our ground-state energies agree within a few percent, while we overestimate the energy of the depolarized system by up to 15%. This is due to the larger correlation energies (ignored in a Hartree-Fock calculation) when two electrons can occupy the same orbital. Since the questions addressed in this paper concern the spin-polarized regime, this deviation from the results of Ref. 7 is of little concern.

The Hartree-Fock approximation is known to conserve symmetries present in the initial trial wave function. To generate deformed solutions, we started with a quite arbitrary, but not rotationally invariant, initial Slater determinant, which produces a deformed initial mean field. Self-consistent

iteration of the Hartree-Fock scheme guarantees amplification of solutions with the symmetry of the Wigner molecule. Of course, the same converged solution must be reached for several different initial states to give confidence that it is the true minimum.

### III. NUMERICAL RESULTS

We have used the material constants of GaAs (i.e.,  $m^* = 0.067m_e$  and  $\epsilon = 12.9$ , as well as an external potential strength of  $\hbar\omega_0 = 3$  meV) for our calculation. To observe the expected phase transition, we first consider a system of  $m=10$  electrons. Figure 1 shows the ground state energy as a function of the magnetic-field strength  $B_0$  and for comparison the lowest energy of the rotationally symmetric system. The Wigner molecule becomes the ground state for  $B_0 \geq 5.2$  T, while at smaller strengths the rotationally symmetric state is favored. The system undergoes spin polarization from  $B_0=0$  T to 1.5 T, where the spin-polarized so-called maximum density droplet<sup>3</sup> prevails. At  $B_0=4.5$  T bulk instabilities result in unoccupied inner Fock-Darwin states. The transition to a Wigner molecule, and later to a crystal,

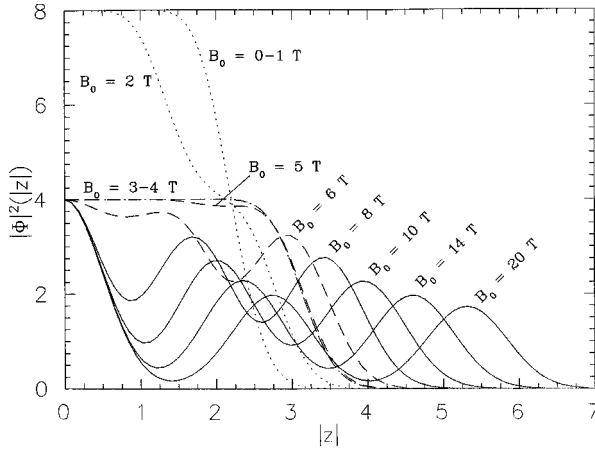


FIG. 3. Radial electron density of  $m=20$  electrons for different values of  $B_0$ . The solid curves represent Wigner crystals, while the dashed curves show the slow transition to a maximum density droplet, which is drawn with a dashed-dotted line. Depolarization sets in for the cases of the dotted curves.

happens very gradually. (We refer to the case where the probability density is deformed, but still very smeared out as a “molecule,” while a “crystal” signifies well localized and distinguishable electrons, as illustrated in Fig. 2.) The molecule at  $B_0=6$  T is lower in energy by only 0.2% (0.542 meV) relative to the rotationally symmetric solution, while the crystal at  $B_0=10$  T gains about  $\sim 3$  meV, which is of order of the strength of the confining potential. Note that the deformed ground states are not eigenstates of the total angular momentum operator  $J = \sum_i \mathcal{L}^{(i)}$ .

The rotationally symmetric case suffers further complication with increasing magnetic-field strength: While at first ( $B_0 \approx 6$  T) the hole in the bulk widens (the  $l=1,2,3$  Fock-Darwin levels empty) and later at  $B_0=6.75$  T a fourth state empties, the solution transforms into two separate rings at  $B_0 \geq 9$  T.

For further insight into the various transitions, the radial (angle-averaged) particle distribution for various magnetic fields is shown in Fig. 3 for  $m=20$  electrons. The crystalline state has one electron in the center of the dot, seven in a middle ring, and 12 electrons in the outermost region. Correspondingly, the  $B_0=20$  T curve shows three maxima. For  $B_0=6$  T the center electron and the seven in the middle ring have almost uniformly merged to a flat distribution, which extends to  $z \approx 2$ , and the outer ring can now be found at  $z \approx 3$ . For  $B_0=3-4$  T we find again the so-called maximum density droplet: the electrons occupy the first 20 Fock-Darwin levels, since they are polarized. Further lowering of  $B_0$  results in a depolarization, allowing further accumulation of electrons near the origin. Since we only take into account  $n=0$  states, we cannot claim to represent the physical situation for the smaller field strength, although we do reproduce the energies in this regime quite well, as noted above.

In Fig. 4 we plot the separation energy  $\Delta(m) = E_{m+1} - E_m$  and the differences in the separation energy,  $\Delta_2(m) = \Delta(m+1) - \Delta(m)$ , as functions of the particle number  $m$  in the crystal regime,  $B_0=20$  T. There is a large drop in  $\Delta_2$  of  $\sim 0.5$  meV whenever charge can be put to the

outer region of the dot (see, e.g.,  $m=4$  and  $m=8$ ), in accord with charge being distributed over a larger area, thereby reducing the Coulomb energy. In the case where one charge is placed in the center and two rings outside ( $m=14$ ), the gain in energy is reduced by the fact that more particles outside feel a stronger external potential. The tendency here is that the Coulomb energy plays a less and less important role, weakening the slope in the separation energy, combined with the fact that one can pack more particle in the outer region.

For comparison, we also show in Fig. 4  $\Delta(m)$  and  $\Delta_2(m)$  for the lowest rotationally symmetric state. No clear tendency in the behavior of  $\Delta_2(m)$  is evident. The system is frustrated by the particles having to occupy Fock-Darwin levels.

In Table I we show the spatial configurations of the system in the Wigner-like structure (obtained by enumerating the number of electrons occupying the corresponding rings) and give the ground-state energies. We generally confirm the configurations of the classical calculation of Ref. 5 as well as the exceptional behavior of the  $m=6, 10, 12$ , and  $17$  clusters, although there is no peak in  $\Delta_2$  for  $m=14$  (the peaks in Fig. 4 correspond to the cusps of Fig. 5 of Ref. 5), since ten electrons are moved outside for the  $m=16$  configuration.

The Hartree Fock calculation is based on a theory of independent particles moving in an average potential. We improved the wave functions for the Wigner regime to a many-body wave function by introducing a Jastrow-type function:

$$|\Psi\rangle = \left( \mathcal{S} \prod_{i < j} f(z_i - z_j) \right) \Phi_{\text{HF}}, \quad (8)$$

where  $\mathcal{S}$  is the symmetrizer and  $\Phi_{\text{HF}}$  the Hartree-Fock solution to the problem. To guarantee a convenient symmetrized form of the product of these function, we made the ansatz

$$f(z_i - z_j) = |z_i - z_j|^k \quad (9)$$

for the pair correlation function  $f(z_i - z_j)$  with  $k$  as a variational parameter. We performed a variational Monte Carlo calculation<sup>8</sup> to evaluate the energy

$$E[k] = \frac{\langle \Psi | H | \Psi \rangle}{\langle \Psi | \Psi \rangle}. \quad (10)$$

As it turned out, the Jastrow type wave function did not significantly improve the Hartree-Fock energy. In the case of ten electrons and  $B=20$  T, the energy could only be improved by 0.1% (0.4 meV) at  $k=0.1$ . For  $0.1 < k < 1$  the energy is slowly increasing, while for  $k > 1$  highly excited states are simulated as more holes are introduced into the wave function. Obviously, the Hartree-Fock solution already describes the Wigner state accurately.

In Fig. 5 we plot the phase diagram with respect to number of particles and the ratio  $\omega_c / \omega_0$ . We omit the regime of bulk instabilities, since it is of minor importance. The phase boundary of the spin-polarized regime and the partially unpolarized regime suffers again from the Hartree-Fock ap-

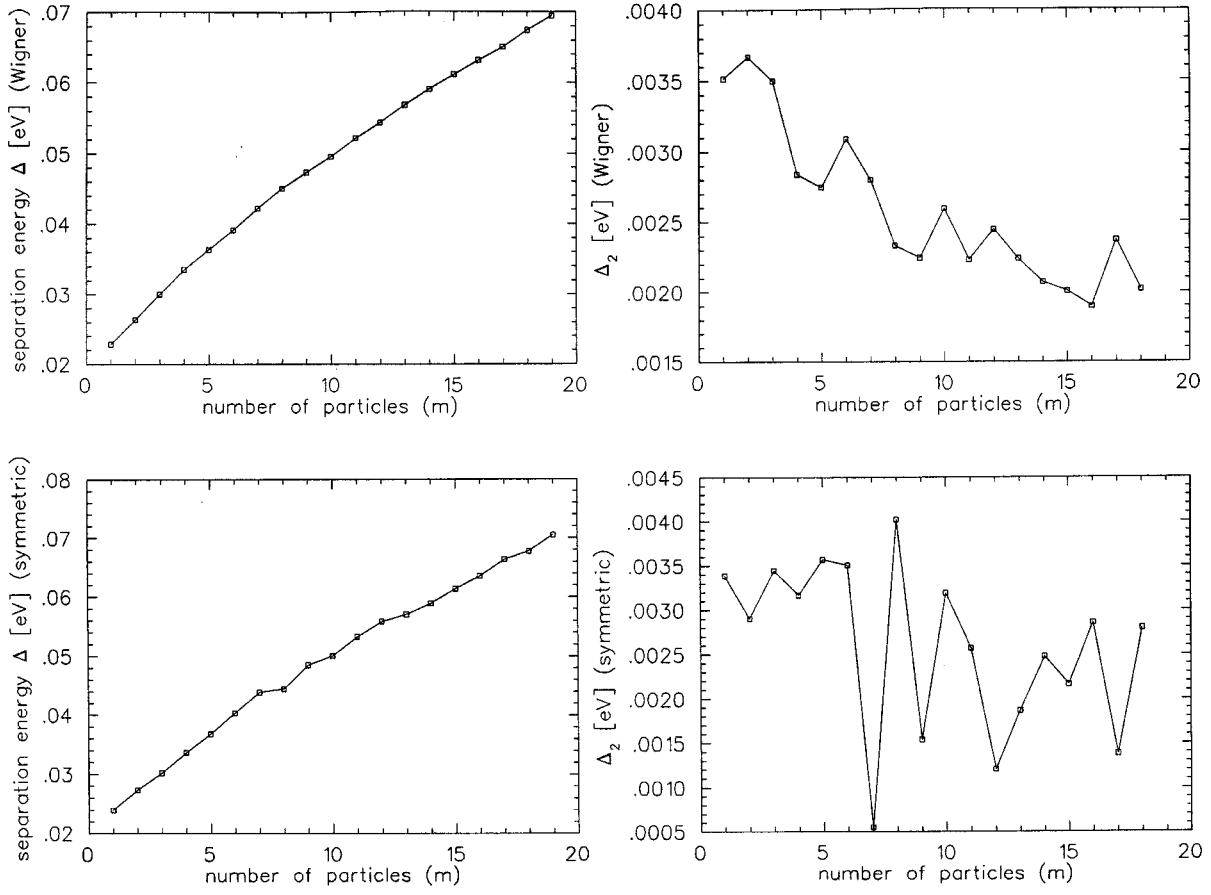


FIG. 4. Separation energy  $\Delta(m)$  and the differences in the separation energy  $\Delta_2(m)$  for Wigner molecules (upper two diagrams) and for the lowest available rotationally symmetric states (lower two diagrams).

proximation, as it bends down with decreasing number of electrons. The boundary of the molecular regime is defined by how much the continuous rotational symmetry is broken: the fractional uncertainty in the total angular momentum is  $f = \Delta J / \langle \hat{J} \rangle = \sqrt{\langle \hat{J}^2 \rangle - \langle \hat{J} \rangle^2} / \langle \hat{J} \rangle$ , and we define a molecule by  $f > 1\%$ . The boundary is fairly constant for  $m > 6$ , but, since the transition is gradual, it has some uncertainty. For less than eight particles, we find a small drop in the boundary, due either to some nonobvious physical effect or to the approximation we use.

In our Hartree-Fock solutions of ten or more electrons and  $B_0 = 20$  T, the relative uncertainty in total angular momentum,  $f$ , is of order of 10%. As in atomic nuclei, these deformed solutions give rise to rotational spectra, which do not appear in the case of the unbroken symmetry. We have estimated the spectrum of rotational excitations by projecting the Hartree-Fock Slater determinant onto eigenfunctions of good angular momentum  $I$ .<sup>9</sup> The projector has the form

$$\hat{P}^I = \frac{1}{2\pi} \int_0^{2\pi} e^{i\alpha(\hat{J}-I)} d\alpha \quad (11)$$

and the energies that result from taking the mean value of  $\hat{H}$  with the projected wave functions are given by

TABLE I. Ground-state energies and spatial distributions of Wigner crystal in quantum dots for up to 20 electrons at  $B = 20$  T.

Number of electrons	Energy (meV)	Ring occupations inner-middle-outer
1	17.247	1-0-0
2	40.085	2-0-0
3	66.439	3-0-0
4	96.463	4-0-0
5	129.986	5-0-0
6	166.346	1-5-0
7	205.448	1-6-0
8	247.636	1-7-0
9	292.621	2-7-0
10	339.934	2-8-0
11	389.489	3-8-0
12	441.634	3-9-0
13	496.008	4-9-0
14	552.825	4-10-0
15	611.879	5-10-0
16	673.004	1-5-10
17	736.135	1-5-11
18	801.162	1-6-11
19	868.558	1-6-12
20	937.973	1-7-12

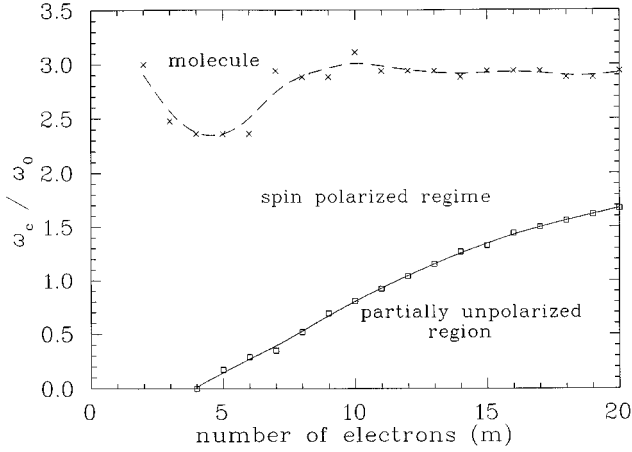


FIG. 5. Phase diagram for quantum dots, plotting  $\omega_c/\omega_0$  vs the number of electrons ( $m$ ). The lines crudely trace the boundaries to guide the eye.

$$E_{\text{proj}}^I = \frac{\langle \Phi | \hat{H} \hat{P}^I | \Phi \rangle}{\langle \Phi | \hat{P}^I | \Phi \rangle} = \frac{\int d\alpha h(\alpha) e^{-i\alpha}}{\int d\alpha n(\alpha) e^{-i\alpha}}, \quad (12)$$

defining the quantities  $h(\alpha) = \langle \Phi | \hat{H} e^{i\alpha \hat{J}} | \Phi \rangle$  and  $n(\alpha) = \langle \Phi | e^{i\alpha \hat{J}} | \Phi \rangle$ . Since the standard deviation in  $\hat{J}$  is only of few percent, one can calculate these matrix elements approximately by writing  $h(\alpha)$  in the expansion

$$h(\alpha) = \sum_{n=0}^K h_n \left( -\langle \hat{J} \rangle + \frac{1}{i} \frac{\partial}{\partial \alpha} \right)^n n(\alpha). \quad (13)$$

One justifies this ansatz with the fact that it represents a Taylor expansion of the Fourier transformed function  $h(\alpha)/n(\alpha)$ , and, assuming that both quantities are sharply peaked at  $\alpha=0$ , this quotient is smooth and can be approximated by a few terms of Eq. (13). By operating  $[\langle -\hat{J} \rangle + (1/i)\partial/\partial\alpha]$  on Eq. (13) and setting  $\alpha=0$ , one gets an inhomogeneous system of equations for the unknown  $h_0, \dots, h_K$ :

$$\langle H(\Delta \hat{J})^m \rangle = \sum_{n=0}^K h_n \langle (\Delta \hat{J})^{m+n} \rangle. \quad (14)$$

Equation (12) can then be expressed as

$$E_{\text{proj}}^I = \sum_{n=0}^K h_n (I - \langle \hat{J} \rangle)^n. \quad (15)$$

We restrict ourselves to  $K=2$ , since higher terms involve the calculation of  $k$ -body operators with  $k>4$ . For this case, we have

$$h_2 = \frac{\langle \Delta \hat{J}^2 \rangle \langle \hat{H} \Delta \hat{J}^2 \rangle - \langle \Delta \hat{J}^3 \rangle \langle \hat{H} \Delta \hat{J} \rangle - \langle \Delta \hat{J}^2 \rangle^2 \langle \hat{H} \rangle}{\langle \Delta \hat{J}^2 \rangle \langle \Delta \hat{J}^4 \rangle - \langle \Delta \hat{J}^3 \rangle^2 - \langle \Delta \hat{J}^2 \rangle^3},$$

$$h_1 = \frac{\langle \hat{H} \Delta \hat{J} \rangle}{\langle \Delta \hat{J}^2 \rangle} - h_2 \frac{\langle \Delta \hat{J}^3 \rangle}{\langle \Delta \hat{J}^2 \rangle}, \quad (16)$$

$$h_0 = \langle \hat{H} \rangle - h_2 \langle \Delta \hat{J}^2 \rangle.$$

Figure 6 shows the rotational spectra for  $m=10$  and  $m=20$  electrons and  $B=20$  T as a function of the quantum number  $I$ , where we have subtracted the shifted ground-state energy, which is obtained from the Hartree-Fock energy  $\langle \hat{H} \rangle$  by subtracting the spurious rotational energy  $h_2 \langle \Delta \hat{J}^2 \rangle$ , which is only of order 0.25 meV in both cases. The moments of inertia associated with these states are  $J_Y = 1/2h_2 = 5.2 \times 10^5 \hbar^2 / \text{eV}$  for  $m=10$  and  $J_Y = 1.9 \times 10^6 \hbar^2 / \text{eV}$  for  $m=20$ .

In order to excite a molecule with circular polarized radiation, one has to produce photons of minimal energy of  $\Delta E^{(10)}(I=224) = E_{\text{proj}}^I(I=224) - (\langle \hat{H} \rangle - h_2 \langle \Delta \hat{J}^2 \rangle) = 1.12 \times 10^{-7}$  eV for the ten electron molecule and  $\Delta E^{(20)}(I=790) = 3.2 \times 10^{-8}$  eV for 20 electrons, which are the energy differences between ground and first excited state. These energies correspond to radio frequencies of  $\nu^{(10)} = 27.06$  MHz and  $\nu^{(20)} = 7.73$  MHz. Note that the corresponding wavelengths are in the transparent region for GaAs. Therefore the measurement of transmission coefficients of circular polarized radiation should give experimental evidence of Wigner molecules. The level spacing,  $\Delta E \approx (\partial E_{\text{proj}}^I / \partial I) \Delta I$ , of the excited states then increases with higher states, resulting in excitations in the microwave region. The heat capacity connected with this rotational degree of freedom,

$$c = \frac{\partial \langle U \rangle}{\partial T} = \frac{\partial}{\partial T} \frac{1}{Z} \left[ \sum_I E_{\text{proj}}^I \exp\left(-\frac{E_{\text{proj}}^I}{k_B T}\right) \right], \quad (17)$$

where  $Z = 1 + \sum_I \exp(-E_{\text{proj}}^I/k_B T)$  is the partition function and  $k_B$  Boltzmann's constant, should therefore reach its classical value of  $\frac{1}{2}k_B$  even for temperature as low as 1 K. Figure 7 shows the well-known Schottky anomaly of the heat capacity, typical for a system where only two states are of importance, at low temperatures of  $\sim 1$  mK. As expected, it approaches  $\frac{1}{2}k_B$  for high temperatures. For the indicated temperature regime the heat capacity has converged within our model space, which consists of 400 rotational states and shows the expected typical behavior of a quantum mechanical rotor in a heat bath.

The energy levels of the vibrational modes of a single electron in the crystal can be estimated in a simplified one-dimensional model. Concerned only with the radial degree of freedom, an outer electron (in the case of ten electrons) interacts with the external potential and the Coulomb potential of the two inner electrons, which we regard positioned at the center:

$$V(r) = \frac{1}{2} m^* \omega_0^2 r^2 + \frac{2e^2}{\epsilon r}. \quad (18)$$

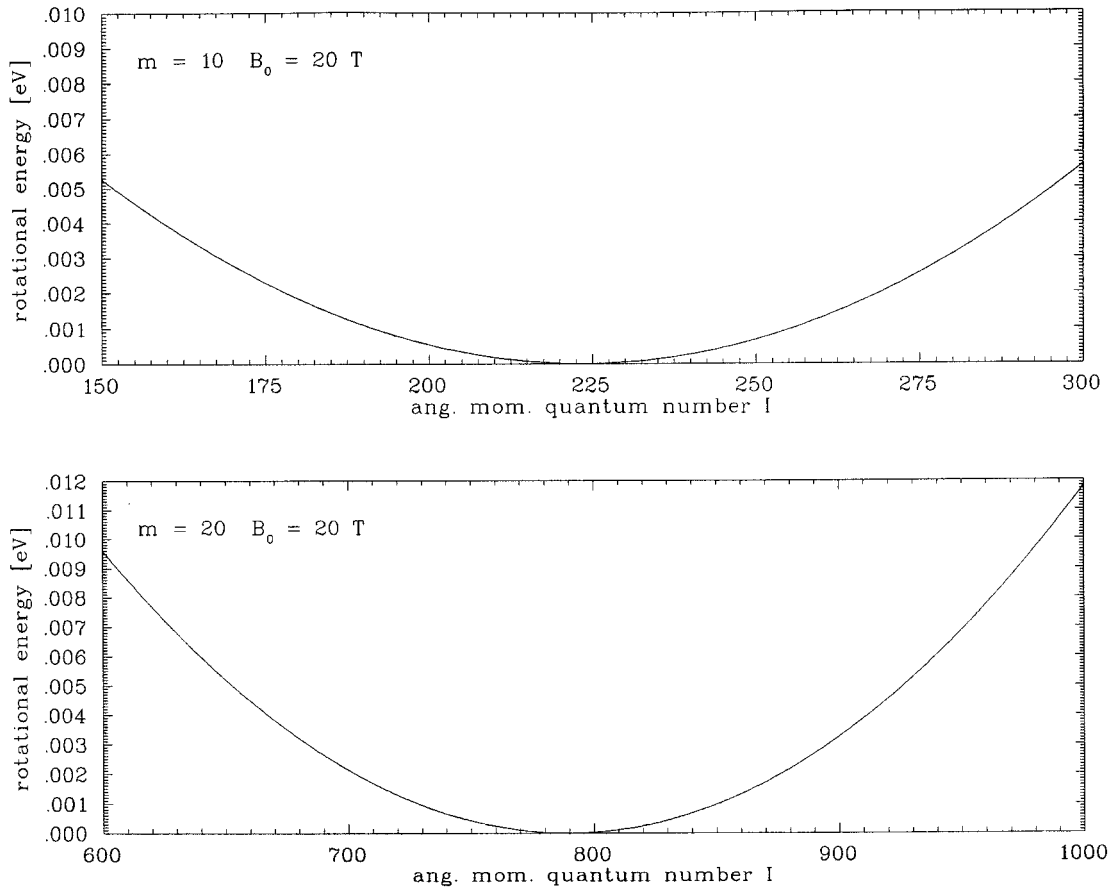


FIG. 6. Rotational spectra for ten electrons (upper diagram) and 20 electrons (lower diagram), when they have formed Wigner molecules at  $B_0=20$  T, as a function of total angular momentum  $l$ .

Expanding the potential around the equilibrium position  $r_0$  of the outer electron to second order, we obtain

$$V(r) = \frac{1}{2} m^* \left\{ \omega_0^2 + \frac{8e^2}{\epsilon m^* r_0^3} \right\} (r - r_0)^2 + \left\{ m^* \omega_0^2 r_0 - \frac{2e^2}{\epsilon r_0^2} \right\} \times (r - r_0) + \frac{1}{2} m^* \omega_0^2 r_0^2 + \frac{2e^2}{\epsilon r_0}. \quad (19)$$

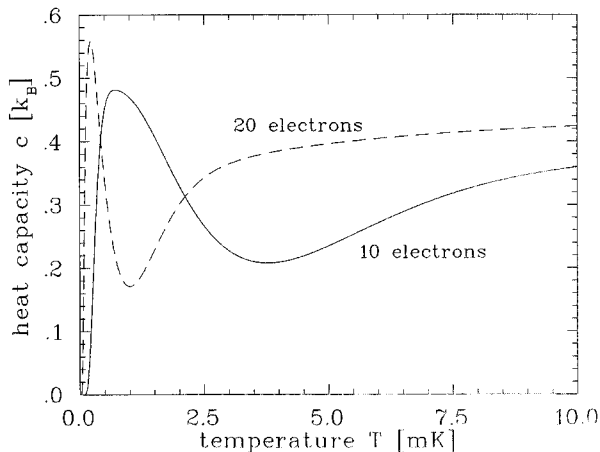


FIG. 7. Heat capacity  $c$  arising from the rotational spectra of Fig. 6. The dashed line shows the 20 electron system, the solid one the ten electron case.

The electron is confined by the parabolic part of this expansion with a corrected strength  $\omega' = \sqrt{\omega_0^2 + 8e^2/\epsilon m^* r_0^3}$ . Setting  $r_0 \approx 2 \times 10^{-6}$  cm, the energy levels for the vibrational modes of the electron are separated by  $\Delta E_{\text{vib}} = \hbar \omega(B_0) = \sqrt{(\hbar \omega')^2 + \frac{1}{4}(\hbar \omega_c)^2} \approx 21$  meV, much larger than the separation in the rotational energy levels ( $\Delta E_{\text{rot}} \approx 10^{-4}$  meV around  $l=225\hbar$ ). Vibrational modes therefore contribute only marginally to the heat capacity and can be easily suppressed by proper excitation of the rotational modes only.

In summary, we have shown in a full quantum mechanical treatment that there exist regimes where Wigner molecules and crystals are the ground states of quantum dots. We have also described rotational spectra of quantum dots, which arise from the existence of deformed Hartree-Fock solutions. This broken symmetry could make it possible to detect Wigner molecules experimentally by exciting the rotational excited states of the system. Open questions remain: How do the two-body correlations neglected in the Hartree-Fock approximation influence systems of few electrons ( $m < 5$ ) and what kind of state is formed in the case of many particles ( $m > 40$ )?

#### ACKNOWLEDGMENTS

This work was supported in part by the National Science Foundation, Grants No. PHY94-12818 and No. PHY94-20470. We thank Karlheinz Langanke and Ming Chung Chu for helpful discussions.

- <sup>1</sup>B.L. Johnson and G. Kirzenow, *Phys. Rev. B* **47**, 10 563 (1993).
- <sup>2</sup>P.A. Maksym, *Physica B* **184**, 385 (1993).
- <sup>3</sup>A.H. MacDonald, S.R. Eric Yang, and M.D. Johnson, *Aust. J. Phys.* **46**, 345 (1993).
- <sup>4</sup>C. de C. Chamon and X.G. Wen, *Phys. Rev. B* **49**, 8227 (1994).
- <sup>5</sup>F. Bolton and U. Rössler, *Superlatt. Microstruct.* **13**, 139 (1992).
- <sup>6</sup>D. Pfannkuche, V. Gudmundsson, and P. A. Maksym, *Phys. Rev. B* **47**, 2244 (1993).
- <sup>7</sup>F. Bolton, *Solid State Electron.* **37**, 1159 (1994).
- <sup>8</sup>J.A. Carlson and R.B. Wiringa, in *Computational Nuclear Physics I*, edited by K. Langanke, J.A. Maruhn, and S.E. Koonin (Springer-Verlag, Berlin, 1991).
- <sup>9</sup>P. Ring and P. Schuck, *The Nuclear Many-Body Problem* (Springer-Verlag, Heidelberg, 1980), p. 466ff.